Sustainable Food Technology

ROYAL SOCIETY OF CHEMISTRY

PAPER

View Article Online
View Journal | View Issue

Cite this: *Sustainable Food Technol.*, 2026, 4, 2862

Portable smartphone enabled colorimetric detection of tetracycline in commercial milk samples *via* peroxidase-mimicking ZnO–Pd nanobolts

Ekta Arjundas Kukreja and Ravi Mani Tripathi *

Tetracyclines (TETs) are widely used broad spectrum antibiotics with low molecular weight. However, excessive use of these bacteriostatic agents has led to their residual increase in the food chain. The presence of TET residues adversely affects human health and the environment. For the detection of trace amounts of antibiotics, the development of ultrasensitive methods is essential. Herein, we have studied the activity of ZnO–Pd nanobolts for the detection of TET. The detection assay was based on the peroxidase mimetic ability of the nanozyme to oxidise a chromogenic substrate 3,3′,5,5′-tetramethylbenzidine (TMB) in the presence of hydrogen peroxide. By the activity of nanozyme the colorless TMB got oxidised into blue color ox-TMB. A turn-off approach was adopted for the detection of TET. In this process, oxidation of TMB was restricted in the presence of TET. The increasing concentrations of TET led to the disappearance of the blue color. The reactions were carried out under optimized conditions. The sensitivity of the assay was evaluated over a range of 0.001–102.4 μM. The specificity of the developed detection assay was analysed by testing various serum interfering analytes along with TET. All the reaction assays were evaluated using the absorbance values obtained by UV-Vis spectroscopy. The LOD and LOQ of the assays were reported to be 0.0029 μM and 0.0087 μM respectively. The relationship between the intensity and the increasing concentrations of TET was also studied using a smartphone, by evaluating the RGB values of the captured images.

Received 26th July 2025
Accepted 7th February 2026

DOI: 10.1039/d5fb00428d

rsc.li/susfoodtech

Sustainability spotlight

The developed colorimetric sensor offers a sustainable, nanozyme powered rapid, specific, and sensitive detection of tetracycline residues in milk samples. Using highly stable and cost-effective ZnO–Pd nanobolts, the method replaces traditional enzyme-based assays, reducing dependence on fragile biological components and harmful substances. The colorimetric response empowers on-site detection without the requirement of sophisticated instruments, and smartphone integration offers user-friendly, portable analysis. This method promotes food safety, reduces environmental impact, and supports low-resource settings by offering a reasonable and scalable solution. Aligning with UN Sustainable Development Goals 3 (Good Health and Well-being) and 12 (Responsible Consumption and Production), our colorimetric assay contributes to safer food monitoring and more sustainable analytical practices.

1. Introduction

Tetracyclines (TETs) are a group of antibiotics with efficient bactericidal activity and low side effects. They are extensively used in treatment of bacterial diseases for both humans and livestock purposes.[1] Misapplication and overexploitation of these antibiotics has led to exposure of TET residues in dietary products prompting gastrointestinal infections and amplifying liver toxicity in humans and other contrary conditions.[2] TET is not completely susceptible to environmental factors which cause only partial degradation of the antibiotic resulting in its long-term persistence in the ecosystem.[3] Hence, it is of great importance to have specific methods for the detection of TET with an efficiency to detect nano-molar concentrations.

Various analytical methods such as immunochromatography assay,[4] high-performance liquid chromatography (HPLC),[5] mass spectrometry,[6] microbial methods[7] and liquid chromatography combined with spectrofluorometric and mass spectrometry[8] are accurate but also have shortcomings such as requirement of operational expertise, sophisticated equipment, prolonged detection time, non-portability, tedious sample preparation and exorbitant costs.[2]

Numerous biosensors have been fabricated for rapid detection of TET including electrochemical,[9] fluorescent[10] and chemiluminescent[11] sensors but they suffer from disadvantages like the usage of hazardous chemicals for generating fluorescence and encumbered electrode processing. Colorimetry is

Amity Institute of Nanotechnology, Amity University Uttar Pradesh, Noida-201301, Uttar Pradesh, India. E-mail: rmtripathi@amity.edu

a technique that addresses these issues and has drawn widespread notice.[12,13] Multitudinous assays including detection of antibiotics,[14,15] glucose,[16,17] heavy metals,[18,19] H_2O_2,[20,21] uric acid[22] *etc.* have fostered the use of colorimetry acknowledging the technique's efficiency and swiftness. Recently, several effective and feasible colorimetric sensors have been reported but they frequently encounter constraints involving tedious preparations, practical applicability and susceptibility to environmental conditions.[2,23] Therefore, there is an acute need to design robust, expeditious and simple biosensors.

For colorimetric sensing, enzymes are of critical functional significance. Natural enzymes are high-priced biological reagents possessing high catalytic properties and substrate specificity, but outrageous environmental conditions tend to cease their catalytic activity.[20] Lately, intensified studies are being conducted on formulating novel nanomaterials with high catalytic activity. These nanomaterials are known to mimic natural enzymes and thus are called nanozymes.[24] In comparison to natural enzymes, nanozymes are robust, economical and possess better catalytic activity with flexibility for modifications.[25] Exceptional enzymatic activity has been reported for numerous nanomaterials such as metal organic nanoparticles,[12,22] carbon nanomaterials,[26,27] noble metal nanoparticles,[28] metal oxide nanoparticles[29,30] and functional polymers.[24]

Zinc oxide (ZnO) is a meticulously studied metal oxide nanomaterial and has gained substantial attention due to its unique physical and chemical properties. The use of ZnO nanostructures is prevalent in applications like biosensing, antibacterial, catalysis, optoelectronics, *etc.* The catalytic activity of ZnO nanostructures is mainly influenced by properties like electron trapping, formation of defects, charge transfer, strong metal–ZnO interaction, *etc.*[31] Moreover, the catalytic activity of ZnO nanomaterials can be enhanced by formulating ZnO based nanocomposites.[32] Pd nanoparticles also show remarkable catalytic activity,[33] but agglomeration of the nanoparticles reduces their catalytic properties.[34] Therefore, a ZnO–Pd nanocomposite material was designed to avert agglomeration of Pd nanoparticles and obtain a highly effective nanozyme. The nanozymatic activity is significantly impacted by the morphology of the nanomaterial. Biological methods of synthesis are recognised for generating nanomaterials with unique morphologies and amplified catalytic activity. Consequently, ZnO–Pd nanoparticles were biologically synthesized using a 'one-pot' strategy demonstrating a nanobolt-like morphology.[35]

This study proposes the use of peroxidase mimetic activity of biologically synthesized ZnO–Pd nanobolts for the detection of TET. The nanocomposite material was engineered using a leaf extract of *E. canadensis*, exhibiting outstanding catalytic activity. The method involved oxidation of a chromogenic substrate-TMB in the presence of H_2O_2 by the activity of the nanozyme. TMB was converted to ox-TMB producing a blue color. It was established that nanobolts possess effective peroxidase mimetic activity that instantly oxidizes TMB. It was noted that the color of the reaction mixture faded in the presence of TET. A significant decrease in the intensity of the color was observed with increasing concentrations of TET. The effect of TET was evaluated over a range of 0.001–102.4 μM. Using UV-Vis spectroscopy, absorbance values at a wavelength of 652 nm were noted and analysed. Furthermore, smartphone analysis was also carried out to investigate the functional utility of the assay. The RBG values were calculated using a smartphone application and the intensity of the color was calculated. The relationship between color intensity and different TET concentrations was studied. Additionally, to augment the reliability of the method real sample analysis was performed by spiking different concentrations of TET in milk samples and examining the absorbance values.

2. Experimental procedures

2.1. Materials

Palladium(II) chloride, zinc acetate dihydrate and 3,3′,5,5′-tetramethylbenzidine (TMB) were procured from Sigma-Aldrich. Sodium acetate, hydrogen peroxide, and acetic acid were purchased from Merck Ltd. Urea, zinc chloride, calcium chloride and H_2O_2 were sourced from Merck. All remaining chemicals were of analytical grade and were used without modifications. A commercial pharmaceutical formulation of tetracycline was used for the study. Packaged milk of a recognised dairy brand was purchased from the local market. The milk brand uses a standard protocol for pasteurization involving heating and chilling procedures at varied temperatures providing a standard shelf life of 48 hours. For the current study, procured milk was directly used after dilution.

2.2. Synthesis of ZnO–Pd nanobolts

In our previous study, we established the protocol for biosynthesis of ZnO–Pd nanobolts using the leaf extract of *E. canadensis*.[35] Concisely, a dispersion was prepared by adding DI water to the cleaned leaves in an Erlenmeyer flask. This dispersion was then boiled and filtered to obtain the leaf extract.

ZnO–Pd nanobolts were synthesized using palladium chloride (0.05 M) and zinc acetate dihydrate (0.2 M). The salts were dissolved in DI water and were continuously stirred at 22 °C. After 30 minutes of stirring, 3 mL of as-synthesized leaf extract was added to the solution followed by addition of NaOH (0.2 M). Under these maintained conditions the reaction proceeded for 60 min. The obtained solution was then centrifuged at 3500 rpm for 15 min, and the resulting precipitate was collected and washed multiple times. The precipitate was freeze dried and powdered ZnO–Pd nanobolts were obtained.

2.3. Characterization of ZnO–Pd nanobolts

To ascertain the structural and morphological properties of the synthesized nanobolts several characterization techniques were used. The size distribution profile of nanobolts was evaluated using the dynamic light scattering technique (DLS) (Zetasizer Nano S90 device, Malvern). For determining the spectral properties of the nanobolts UV-Vis spectroscopy (UH-5300, Hitachi, Japan) was performed. X-ray photoelectron spectroscopy (XPS;

Thermo Scientific, UK) was employed to deduce the oxidation state of Pd. To study the crystallinity of the nanomaterial X-ray diffractometry (XRD; X'Pert PRO, PANanalytical, Netherlands) was employed. Energy-dispersive X-ray spectroscopy (EDS) along with field-emission scanning electron microscopy (FESEM; Zeiss, EVO 18, Germany) was conducted to determine the elemental and structural characteristics of the nanomaterial. Transmission electron microscopy (TEM; JEM-3010, JEOL, Japan) was carried out for an elaborated study of crystallinity, shape, size and lattice spacing.

2.4. Factors influencing nanozymatic activity

The nanozymatic activity of a nanozyme is influenced by numerous factors such as buffer pH, buffer concentration, nanozyme concentration and incubation time. To obtain the optimal activity of the nanozyme, these factors were calibrated. For optimization of buffer pH, the reaction was carried out at different pH-3.6, 4, 4.6, and 5. The various molarities (0.05 M, 0.1 M, 0.2 M and 0.3 M) of buffer were used to standardize the buffer conditions to obtain high nanozymatic activity of ZnO–Pd nanobolts. The concentration of nanozyme used in the reaction also plays a major role in establishing the optimal working conditions for attaining the paramount peroxidase mimetic activity. Therefore, the activity of nanozyme was studied at different concentrations ranging from 0.025 to 0.1 mg mL^{-1}. Subsequently, the reaction mixture was analysed at different intervals of time to obtain the optimum window of incubation. The reaction mixture was incubated for 1 to 30 minutes and scanned using UV-Vis spectroscopy to analyse the highest absorbance at 652 nm. All the reaction mixtures were incubated at 22 °C as optimized in our previous studies.[36,37]

2.5. Colorimetric detection of TET

The peroxidase mimetic activity of ZnO–Pd nanobolts was employed for the detection of TET. The developed assay uses a chromogenic substrate TMB which gets oxidised by H_2O_2 in the presence of nanozyme. To detect TET, 500 mg of antibiotic was dissolved in DI water, and the reaction was carried out under optimal conditions. The reaction mixture was composed of 1.56 mM of TMB, 1 M of H_2O_2 and 0.025 mg mL^{-1} of nanozyme in acetate buffer of pH 4.6. The reaction mixture was allowed to incubate for 20 minutes at 22 °C. Thereafter, it was scanned using UV-Vis spectroscopy to obtain the absorbance value.

2.6. Sensitivity and specificity

Different concentrations of TET were examined to evaluate the sensitivity of the detection assay. The concentration span used for estimation was 0.001–102.4 μM. Multiple stock solutions with different molarities were formulated for the estimation. The reaction was performed in acetate buffer at 22 °C and the mixture was incubated for 20 minutes. The proportionality relationship between the intensity of assay and the concentrations of TET was studied using absorbance values obtained at 652 nm.

Reactions with TET and various serum and urine interfering analytes (urea, Ca^{2+}, Fe^{3+}, Na^{+}, K^{+}, NH_4^{+}, glucose, tryptophan, lactose, phenylalanine and methionine) were carried out to analyse the specificity of the method. The reaction mixtures were scanned, and the attained UV-Vis spectra were evaluated for determining the specificity of the developed detection method.

2.7. Real sample analysis

To evaluate the practical application of the developed assay real sample analysis was performed. The test was conducted on milk samples procured from the local market. Foregoing the detection of TET, 1 mL milk was diluted 400 times and was spiked with different concentrations of TET using the standard addition approach. These spiked samples were used for the detection of TET. The average recovery rate (%) and relative standard deviation (%) were calculated for each concentration.

3. Results and discussion

3.1. ZnO–Pd nanobolts

Optical properties of ZnO–Pd nanobolts were studied using UV-Vis spectroscopy. In a wide absorption plot, a broad peak at a wavelength of 327 nm was obtained (Fig. S1). A bandgap (E_g) of 2.9 eV was evaluated for nanobolts using the Tauc plot (Fig. S6).

The size determining spectrum was obtained through DLS. The average diameter of the nanobolts was established to be 994.9 nm (Fig. S1). A polydispersity index of 0.338 was recorded for the nanomaterial demonstrating exceptional stability and quality.[35]

The crystalline structure and purity of the ZnO–Pd nanobolts were studied using XRD analysis. The peaks were observed at 2θ values of 31.77°, 34.44°, 36.23°, 47.51°, 56.56°, 62.88°, 66.30°, 67.8°, 69.03°, 72.46°, and 76.86°, coinciding with the (100), (002), (101), (102), (110), (103), (200), (112), (201), (004), and (202) planes, respectively (Fig. S2). As stated by the Joint Committee on Powder Diffraction Standards (JCPDS), it was validated that the data were characteristic of the hexagonal wurtzite structure. The highest intensity peak observed at the (101) plane corresponds to the direction of nanocrystal growth whereas the low-intensity peak recorded at the (111) plane indicates the crystal plane of Pd, confirming the presence of Pd in ZnO–Pd nanobolts.[35]

The oxidation state of Pd in the ZnO–Pd nanobolts was evaluated using XPS data. A binding energy of 335.22 eV was recorded reflecting the 3d spectrum of Pd and suggesting the presence of Pd (0) metal[35] (Fig. S1). It was noted that the properties of the constituents were persistent on mixing ZnO and Pd.

FESEM scans were utilized to examine the morphological properties of the nanomaterial. The structural uniformity was confirmed using the image obtained at 100 00× magnification with a size range from 50 to 287 nm (Fig. S3). It was observed that the average height of the nanobolt was recorded to range from 49 to 83 nm with a 49.8 nm deep hole retained by some nanobolts.[35] The elemental make-up of the ZnO–Pd nanobolts was estimated by EDS. Intensified peaks were observed for Zn, O and Pd validating the formation of ZnO–Pd nanobolts. The EDS analysis was used to estimate the weight percentages and the atomic percentages of Zn, O and Pd[35] (Fig. S4).

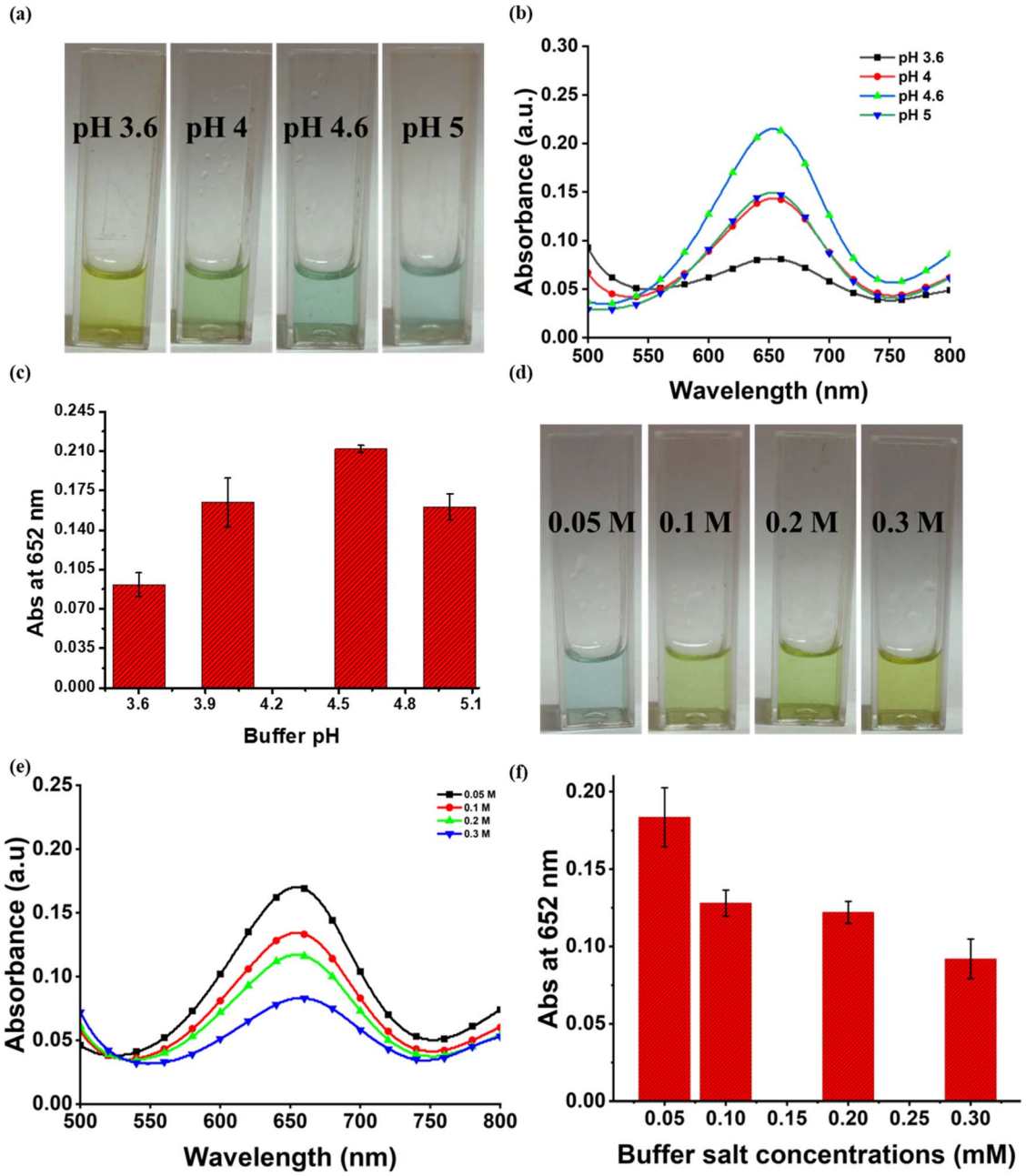

Fig. 1 Influence of buffer pH and buffer concentration. (a) Image showing the effect of buffer pH on the color; (b) absorbance spectra at different pH; (c) effect of pH determined using absorbance values at 652 nm and standard deviation obtained using experimental data, indicated by error bars; (d) the effect of different buffer concentrations on color; (e) absorbance spectra obtained at various buffer concentrations; (f) effect of buffer concentrations determined using absorbance values at 652 nm and standard deviation obtained using experimental data, indicated by error bars.

The nanobolts were analysed using TEM images projecting bolt-like structures analogous to the FESEM results. The TEM results were used for determining the diameter (44.5 nm) and the thickness (13.8–66.6 nm) of the nanomaterial (Fig. S5).

3.2. Detection of TET

The tendency of ZnO–Pd nanobolts to facilitate the oxidation of TMB in the presence of H_2O_2 was exploited for the detection of TET. Due to the peroxidase mimetic activity of nanobolts, TMB is oxidised changing the color of the reaction mixture from colorless to blue. The oxidation of TMB occurs due to the generation of $^{\bullet}OH$ produced by the action of nanozyme on H_2O_2. It was observed that on addition of TET to the reaction mixture the intensity of the blue color was lower than that of the blank assay. This is because the double bonds and phenolic and amine functional groups of TET exhibit high electron density, readily attracting the $^{\bullet}OH$.[38] It was previously reported that the reaction between TET and $^{\bullet}OH$ is favoured over oxidation of TMB by the $^{\bullet}OH$ such that the formation of a covalent bond

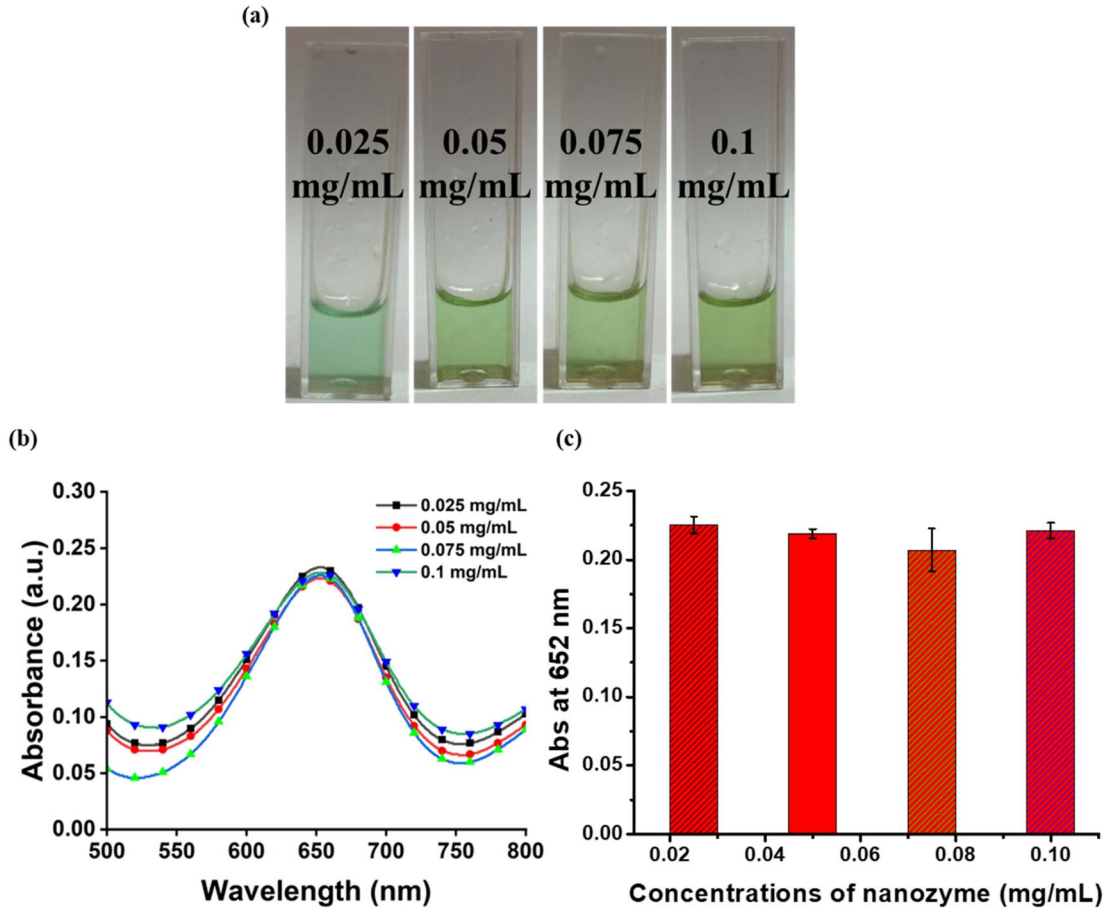

Fig. 2 Influence of nanozyme concentration. (a) The effect of different concentrations of nanozyme on color; (b) absorbance spectra at different nanozyme concentrations; (c) effect of nanozyme concentration determined using absorbance values at 652 nm and standard deviation obtained using experimental data, indicated by error bars.

between TET and $^{\bullet}OH$ inhibits the reaction between $^{\bullet}OH$ and TMB.[3,39] Hence it can be stated that the $^{\bullet}OH$ produced during the reaction shows higher affinity towards TET than towards TMB.

In the study, a range of 0.001–102.4 μM of TET was used for the analysis. The reaction was carried out in acetate buffer of pH 4.6 consisting of 1.56 mM of TMB, 1 M of H_2O_2 and 0.025 mg mL^{-1} of nanozyme with a final volume of 1 mL and the mixture was incubated for 20 minutes. The assay containing TET showed no visible change in the color whereas the blue color of ox-TMB was observed in the blank assay. The reaction mixtures were scanned using UV-Vis spectroscopy over a wavelength of 400 to 800 nm. A strong peak was observed for the blank assay, and no prominent peak was attained for the assay containing TET. Flattening of the absorbance peak was observed with an increase in the concentration of TET. Therefore, it was estimated that increasing concentrations of TET restricted the oxidation of TMB.

3.3. Influence of various conditions

3.3.1. Effect of buffer pH. In a colorimetric reaction, the buffer pH is a vital parameter that determines the peroxidase activity of the nanozyme. Optimal activity of the nanozyme is particularly observed at a specific pH. Reactions were carried out at four different buffer pH. The pH values used in the study were 3.6, 4, 4.6 and 5. Favourable results were observed at pH 4.6 and 5 when observed by the naked eye. However at pH 3.6 and 4, yellow and greenish-blue color of the ox-TMB was observed, respectively. The reaction mixtures were scanned, and the highest absorbance value was obtained at pH 4.6 at a wavelength of 652 nm (Fig. 1), whereas peak intensities for pH 4 and 5 were substantially lower. The lowest absorbance peak was recorded for pH 3.6. Therefore, pH 4.6 was noted to be the optimum pH for the reaction.

3.3.2. Effect of buffer concentration. Buffer concentrations used were studied after optimization of pH. Different molarities ranging from 0.05 M to 0.3 M were used for the preparation of the buffer. The reactions were carried out at each molarity, and the most effective results were noted at 0.05 M buffer concentration when observed visually. At all the other concentrations greenish-blue color of the ox-TMB was recorded. The reaction mixtures were further scanned using UV-Vis spectroscopy. The highest absorbance value was obtained for the 0.05 M concentration (Fig. 1). It was also observed that the catalytic activity of the nanozyme decreased as the buffer concentration was increased. Hence, an inversely proportional relationship was

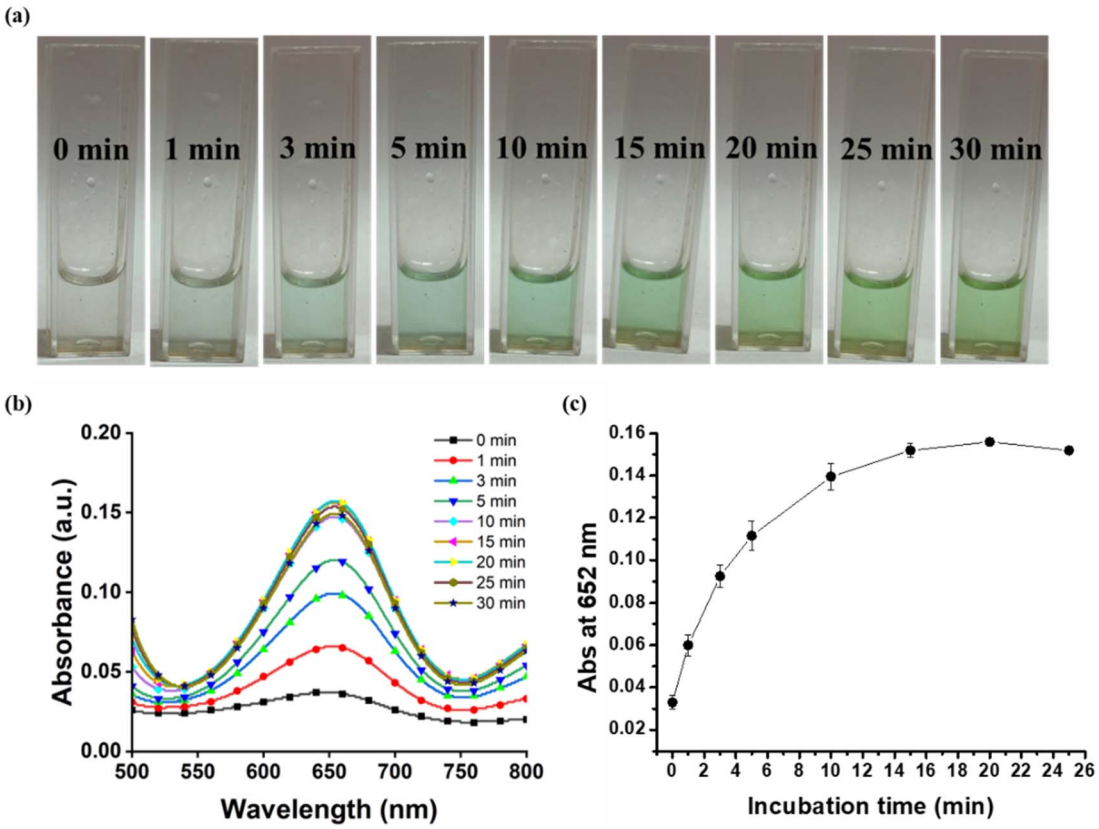

Fig. 3 Influence of incubation time. (a) The variation in color intensity at different time durations; (b) absorbance spectra at different time durations; (c) effect of incubation time determined using absorbance values at 652 nm and standard deviation obtained using experimental data, indicated by error bars.

observed between the ionic concentration of buffer and the catalytic activity.

3.3.3. Effect of nanozyme concentration. For estimation of the optimal nanozyme concentration reactions with different nanozyme concentrations were carried out. The range of concentrations used in the study was 0.025 to 0.1 mg mL^{-1}. Visually, blue color of the ox-TMB was only obtained at 0.025 mg mL^{-1} nanozyme concentration whereas at the remaining concentrations greenish-blue color was obtained (Fig. 2). The solutions were scanned, and the highest value of absorbance was retained at 0.025 mg mL^{-1}. No significant difference was observed in the absorbance values attained for the other concentrations. Consequently, the optimal nanozyme concentration was estimated to be 0.025 mg mL^{-1}.

3.3.4. Effect of incubation time. For determining the ideal incubation time for the developed detection method, the

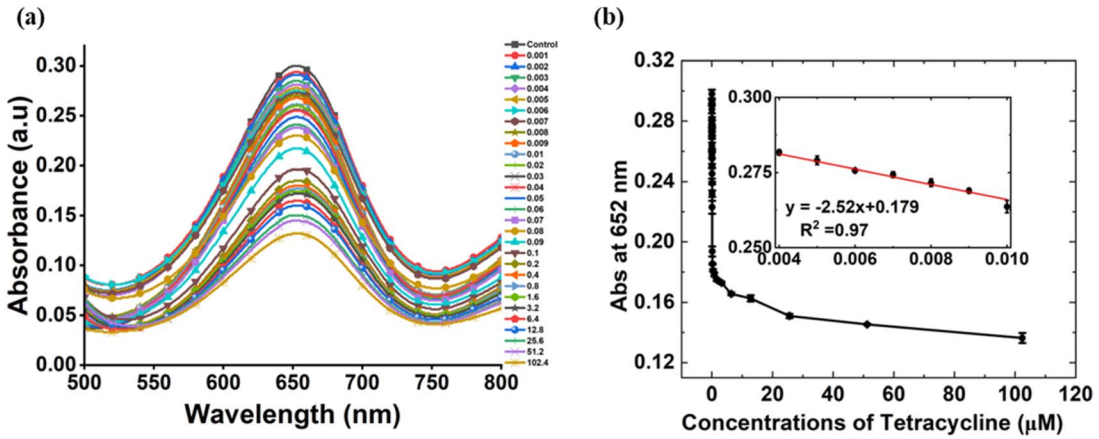

Fig. 4 Sensitivity of the TET detection method: (a) absorbance spectrum studied over a TET concentration range of 0 μM to 102.4 μM. (b) Spectrum between absorbance values obtained at 652 nm and TET concentrations; the inset reflects a linear response at lower concentrations.

Table 1 Comparison of various studies performed for detection of tetracycline

Detection mode	Signal type	Detection limit (nM)	Incubation time (min)	References
Titanium carbide MXene	Colorimetric assay	615.38	10	3
N–C co-doped Fe-based nanoparticles	Colorimetric assay	62	17	1
Ferritin nanoparticles	Colorimetric assay	15.0	30	2
Fe_3O_4 magnetic nanoparticles	Colorimetric assay	45	30	40
Molecularly imprinted sites onto the Fe_3O_4 nanozyme	Colorimetric assay	400	10	41
Copper-based nanoenzyme	Colorimetric assay	270	—	42
Gold nanoclusters	Colorimetric assay	46	90	43
Aptamer modified triple-metal nanozyme	Colorimetric assay	7.1	35	44
ZnO–Pd nanobolts	Colorimetric assay	2.9	20	This study

reaction mixtures were incubated for different time durations. The experiment was carried out at various intervals between 0–25 minutes (Fig. 3). With increasing duration, the intensity of the blue color increased visibly up to 20 minutes. The reaction mixtures were scanned, and analogous results were recorded. A substantial increase in the absorbance values was noted up to 20 minutes. A slight decrease in the absorbance was observed after 20 minutes. Hence, 20 minutes was evaluated to be the most suited incubation time.

3.4. Sensitivity

The merit of a detection assays can be estimated using its sensitivity. The sensitivity of an assay is an essential parameter demonstrating linear response obtained at the lowest concentrations of the analyte in a sample. Herein, sensitivity of the method was established by performing experiments with varying concentrations of TET over a range of 0 to 102.4 μM. Visually, after 20 minutes of incubation, not much difference in the color intensity was observed at the lower concentrations but a significant difference was noted at higher concentrations. No color was observed at 102.4 μM concentration of TET. All the reaction mixtures were scanned on the scale of 400 to 800 nm.

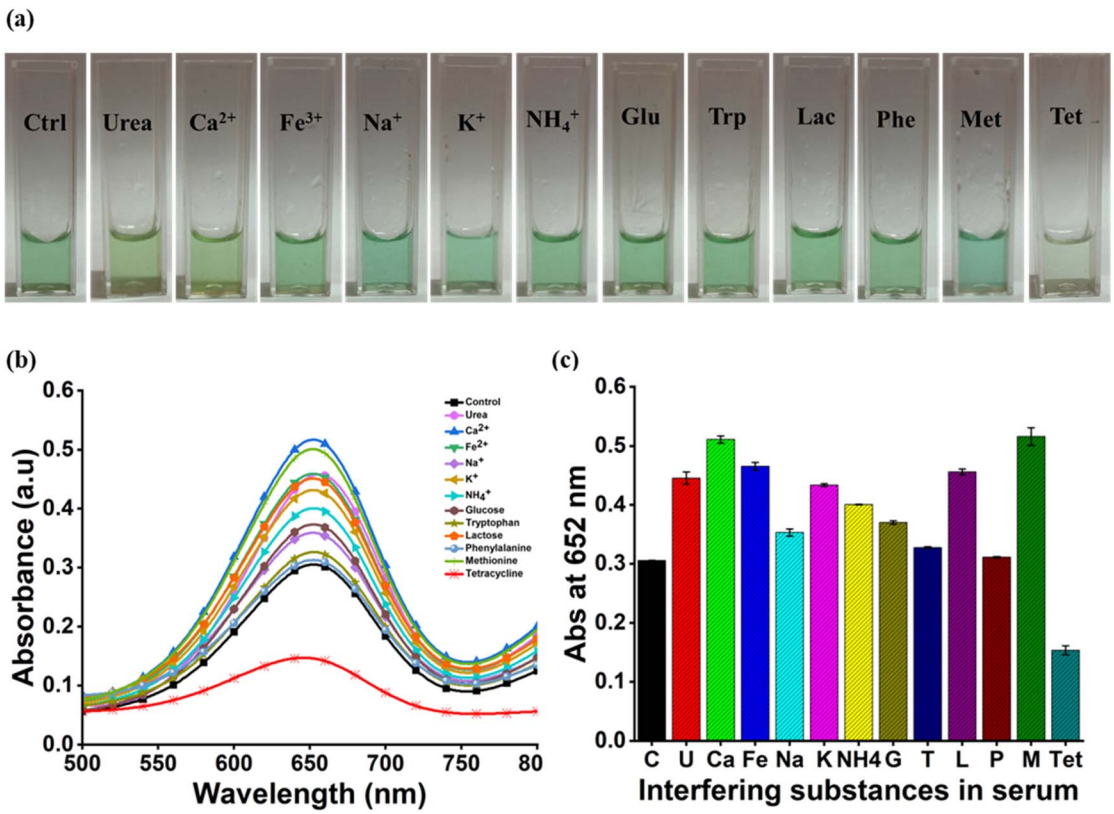

Fig. 5 Specificity of the TET detection method: (a) the color response for TET and all the other analytes. (b) Absorbance spectrum for TET and the other analytes. (c) Spectrum between the absorbance at 652 nm of various serum-interfering substances and standard deviations obtained using experimental data, indicated by error bars.

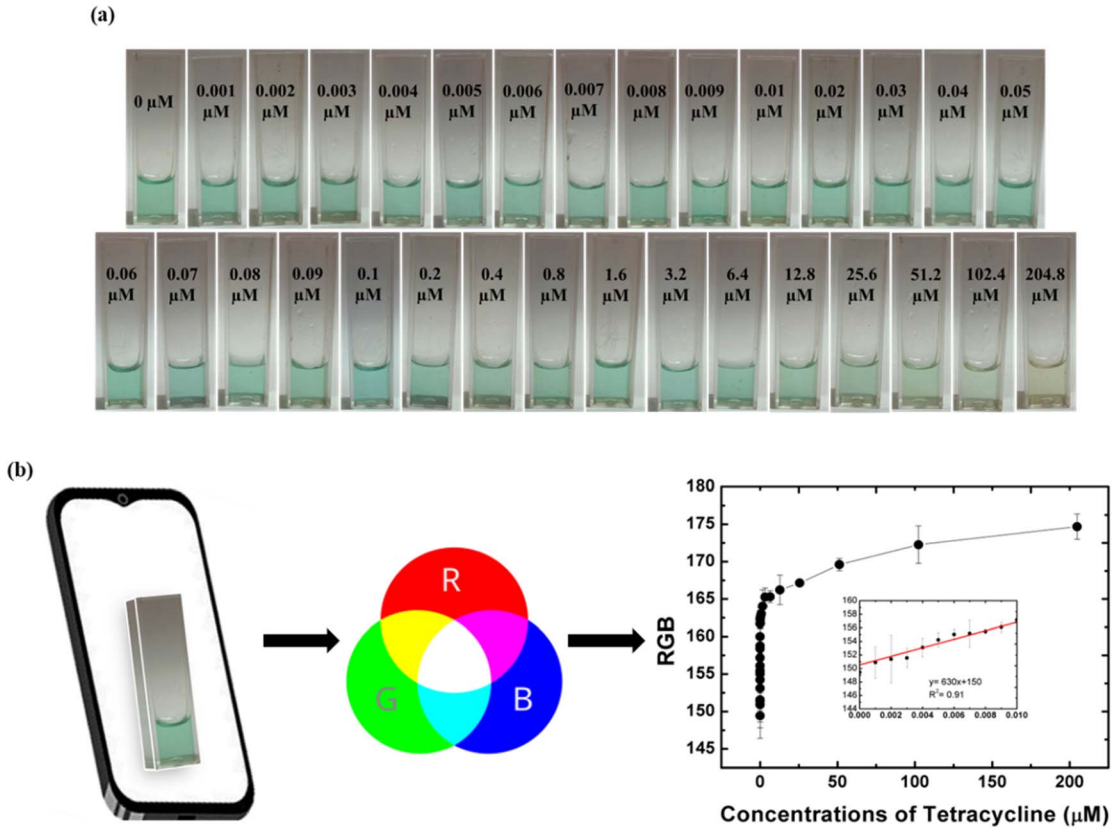

Fig. 6 Smartphone-based study. (a) Changes in the color intensity at different concentrations of TET. (b) RGB analysis using a smartphone and a spectrum depicting the relationship between the intensity and the TET concentrations; the inset demonstrates the linearity at lower concentrations.

The absorbance values were recorded at 652 nm and a consistent decrease in the absorbance was recorded with increasing concentration of TET. A strong peak with the highest intensity was obtained for the blank sample whereas the intensity of the peak noted for the sample containing 102.4 μM of TET was prominently low. The detection method represents a linear regression correlation coefficient of 0.97 at lower concentrations of TET signifying a linear response (Fig. 4). The limit of detection (LOD) and limit of quantification (LOQ) of the method was calculated to be 0.0029 μM and 0.0087 μM respectively. Table 1 shows the comparison of our work with the previously reported studies performed for the detection of TET. The LOD and LOQ were determined using the following equations:

$$\text{LOD} = 3{\cdot}3 \times \text{Standard deviation of the regression line/slope}$$

$$\text{LOQ} = 10 \times \text{Standard deviation of the regression line/slope}$$

3.5. Specificity

Reactions were carried out with TET and various serum interfering analytes including urea, Ca^{2+}, Fe^{3+}, Na^{+}, K^{+}, NH_4^{+}, glucose, tryptophan, lactose, phenylalanine and methionine to evaluate the specificity of the detection method. The determination of specificity is crucial to establish that the developed system successfully distinguishes TET from other analytes under standardised conditions. Independent analysis of each analyte was carried out by adding 100 μM of each to the reaction mixture. After incubation the development of the color was recorded for each assay and the intensities were compared. The disappearance of blue color of the ox-TMB was only observed in the presence of TET and all the remaining mixtures appeared blue. Absorbance spectra of all the analytes were autonomously recorded using UV-Vis spectroscopy from 400 to 800 nm and absorbance values at 652 nm were compared. The lowest absorbance value was obtained for the sample containing TET whereas the absorbance values of all the other analytes were either similar to or greater than that of the blank sample (Fig. 5). This depicts that under optimised conditions only TET shows higher affinity towards $^{\bullet}OH$ than TMB in comparison to the other serum interfering substances. Therefore, it can be concluded that the designed assay is notably specific to TET.

3.6. Smartphone based analysis

Ultrasensitive and specific detection methods are introduced to enhance the quality of diagnosis procedures for speedy and effective detection. Smartphones are the most prevalent devices of modern-day technology. High-tech cameras in smartphones are acceptable gadgets for colorimetry. Hence, smartphone-based analysis is a convenient approach towards development

Table 2 Detection of TET in milk samples

Samples	Added TET (μM)	Found TET (μM)	Recovery (%)	RSD (%, $n = 3$)
Milk	0	0.010	—	—
	50	60.21	120.40	2.45
	100	107.30	107.29	2.83
	200	177.82	88.90	4.95

of sophisticated point-of-care devices. Here, RGB values of the images acquired on a smartphone were obtained using a smartphone application named RGB Color Detector. The values were recorded for respective concentrations and the intensity of color of each sample solution in the image was calculated using the equation $I = 0.3R + 0.59G + 0.11B$.[45] The concentration range adopted for analysis was 0 μM to 204.8 μM (Fig. 6). Identical and consistent lighting conditions were set up for image acquisition of reaction mixtures to decrease the deviations. All images were captured under a closed box to maintain controlled conditions and minimize the influence of ambient light. Uniform illumination was provided using a white LED light source in the box and another very important parameter is the distance between the reaction mixture and smartphone camera which was kept fixed during the visual documentation. Lastly, the parameters of the camera such as focus, exposure, and white balance were identical for all measurements. According to the results, it was noted that the intensity varied linearly with the increasing TET concentrations. A similar relationship was observed at lower concentrations with a linear regression coefficient of 0.91 logged.

3.7. Real sample analysis

To determine the viability and dependability of the study, the presence of TET was estimated in milk samples. The evaluation was carried out using the standard addition method. The milk samples were spiked with 50 μM, 100 μM and 200 μM of TET for the testing. The results in Table 2 show the average recovery rates from 88.90 to 120.40% and relative standard deviation (RSD) in the range of 2.45 to 4.95%. The outcomes of the experiment suggest that the designed colorimetric assay is reliable and has the potential to operate as a precise and specific sensor.

4. Conclusion

In summary, we have effectively demonstrated, for the first time, the application of ZnO–Pd nanobolts for the detection of TET. The nanomaterial was biologically synthesized using a leaf extract obtained from *E. canadensis*. The synthesized nanobolts were found to exhibit high peroxidase mimetic activity. They readily oxidised the chromogenic substrate TMB in the presence of H_2O_2 leading to the production of a blue color. Before the development of the detection assay certain influencing factors were calibrated to attain the maximum peroxidase mimetic activity of the nanozyme. It was noted that oxidation of TMB was abated due to higher affinity of $^{\bullet}OH$ towards TET than to TMB. Therefore, in the presence of TET the blue color of the reaction mixture starts to fade. With increasing TET concentrations, the intensity of the color decreased. The absorbance values of the assays were analysed at 652 nm. The LOD was reported to be 0.0029 μM and LOQ was noted to be 0.0087 μM. Various serum interfering substances were used for the estimation of the specificity of the method. Visually, no color change was observed for TET whereas for all other analytes the appearance of blue color of ox-TMB was observed. The presence of TET in milk was evaluated for assessing the real-time application of the assay. Smartphone-based analysis was also performed for the developed assay. The RGB values were calculated using a smartphone application and a linearity was established between the concentrations of TET and the intensity of the color. The detection assay was proven to be ultra-sensitive and highly specific for the detection of TET.

Author contributions

R. M. T. developed the study concept and contributed to study design. E. A. K. performed the experiments related to peroxidase mimetic activity of ZnO–Pd nanobolts and detection of tetracycline. R. M. T. supervised the whole study. R. M. T. and E. A. K. analysed and discussed the results thoroughly and contributed to the final version of the manuscript. The authors have read and agreed to the published version of the manuscript.

Conflicts of interest

The authors declare that they have no known competing financial interests or personal relationships that could have appeared to influence the work reported in this paper.

Data availability

Data will be made available on request.

Supplementary information (SI) is available. See DOI: https://doi.org/10.1039/d5fb00428d.

Acknowledgements

This research was supported by the Anusandhan National Research Foundation (ANRF), India, *via* Grant TAR/2022/000074.

References

1 W. Wen, Y. Liu, Z. Li, G. Wen, H. W. Li and L. Li, Magnetic Fe–N–C nanoparticles as a dual nanozyme for label-free colorimetric detection of antibiotics, *Environ. Sci. Adv.*, 2023, **2**(5), 731–739, DOI: 10.1039/d2va00319h.

2 Y. Zhu, K. Zhou, R. Sheng, Y. Wang, H. Zhou, K. Cai and B. Xu, A novel biosensor utilizing the peroxidase-like activity of bovine spleen ferritin for highly sensitive detection of tetracycline antibiotics, *J. Food Compos. Anal.*, 2023, **119**, 105277, DOI: 10.1016/j.jfca.2023.105277.

3 W. Wang, Y. Yin and S. Gunasekaran, Nanozymatic degradation and simultaneous colorimetric detection of

tetracycline, *Food Chem.*, 2023, **426**, 136607, DOI: 10.1016/j.foodchem.2023.136607.

4 Y. Xu, B. Ma, E. Chen, X. Yu, C. Sun and M. Zhang, Functional up-conversion nanoparticle-based immunochromatography assay for simultaneous and sensitive detection of residues of four tetracycline antibiotics in milk, *Front. Chem.*, 2020, **8**, 759, DOI: 10.3389/fchem.2020.00759.

5 M. L. Castillo-García, M. P. Aguilar-Caballos and A. Gómez-Hens, A europium-and terbium-coated magnetic nanocomposite as sorbent in dispersive solid phase extraction coupled with ultra-high performance liquid chromatography for antibiotic determination in meat samples, *J. Chromatogr., A*, 2015, **1425**, 73–80, DOI: 10.1016/j.chroma.2015.11.048.

6 I. Dalmázio, M. O. Almeida, R. Augusti and T. M. Alves, Monitoring the degradation of tetracycline by ozone in aqueous medium *via* atmospheric pressure ionization mass spectrometry, *J. Am. Soc. Mass Spectrom.*, 2007, **18**, 679–687, DOI: 10.1016/j.jasms.2006.12.001.

7 C. C. Weber, N. Link, C. Fux, A. H. Zisch, W. Weber and M. Fussenegger, Broad-spectrum protein biosensors for class-specific detection of antibiotics, *Biotechnol. Bioeng.*, 2005, **89**(1), 9–17, DOI: 10.1002/BIT.20224.

8 A. Pena, C. M. Lino, R. Alonso and D. Barceló, Determination of tetracycline antibiotic residues in edible swine tissues by liquid chromatography with spectrofluorometric detection and confirmation by mass spectrometry, *J. Agric. Food Chem.*, 2007, **55**(13), 4973–4979, DOI: 10.1021/jf070398j.

9 A. Mohammad-Razdari, M. Ghasemi-Varnamkhasti, S. Rostami, Z. Izadi, A. A. Ensafi and M. Siadat, Development of an electrochemical biosensor for impedimetric detection of tetracycline in milk, *J. Food Sci. Technol.*, 2020, **57**(12), 4697–4706, DOI: 10.1007/s13197-020-04506-2.

10 S. Han, L. Yang, Z. Wen, S. Chu, M. Wang, Z. Wang and C. Jiang, A dual-response ratiometric fluorescent sensor by europium-doped CdTe quantum dots for visual and colorimetric detection of tetracycline, *J. Hazard Mater.*, 2020, **398**, 122894, DOI: 10.1016/j.jhazmat.2020.122894.

11 C. Li, C. Zeng, Z. Chen, Y. Jiang, H. Yao, Y. Yang and W. T. Wong, Luminescent lanthanide metal-organic framework test strip for immediate detection of tetracycline antibiotics in water, *J. Hazard Mater.*, 2020, **384**, 121498, DOI: 10.1016/j.jhazmat.2019.121498.

12 A. Deshwal, R. M. Tripathi, K. Saxena, F. A. Sheikh and P. Mishra, Auriferous nanozymes: advances in diagnostic and therapeutic applications, *Nanotechnology*, 2024, **35**(50), 502003, DOI: 10.1088/1361-6528/ad7f5d.

13 A. Deshwal, K. Saxena, G. Sharma, F. A. Sheikh, C. S. Seth and R. M. Tripathi, Nanozymes: a comprehensive review on emerging applications in cancer diagnosis and therapeutics, *Int. J. Biol. Macromol.*, 2024, **256**, 128272, DOI: 10.1016/j.ijbiomac.2023.128272.

14 A. Mishra, E. A. Kukreja, R. N. Pudake, R. Kumar, M. P. Singh, L. Yadav, I. Pandey, F. A. Sheikh and R. M. Tripathi, Label-free selective and sensitive colorimetric detection of ampicillin in milk and water using silver nanoparticles, *J. Food Compos. Anal.*, 2023, **119**, 105256, DOI: 10.1016/j.jfca.2023.105256.

15 N. Sethu, S. Krishnakumar, V. Mitra, C. Tagad and R. Vyas, Design and development of a novel colorimetric assay and a portable optical system for the detection of aminoglycoside antibiotics, *Sens. Acutators Rep.*, 2023, **5**, 100151, DOI: 10.1016/j.snr.2023.100151.

16 S. Ghateii and A. Jahanshahi, Colorimetric detection of glucose with smartphone-coupled μPADs: Harnessing machine learning algorithms in variable lighting environments, *Sens. Actuators, B*, 2024, **400**, 134835, DOI: 10.1016/j.snb.2023.134835.

17 T. Chen, Y. Jiang, Y. Wu, M. Lai, X. Huang, Z. Gu, J. Wu, Y. Gan, H. Chen, W. Zhi and P. Sun, Doughnut-shaped bimetallic Cu–Zn-MOF with peroxidase-like activity for colorimetric detection of glucose and antibacterial applications, *Talanta*, 2024, **279**, 126544, DOI: 10.1016/j.talanta.2024.126544.

18 R. M. Tripathi, S. H. Park, G. Kim, D. H. Kim, D. Ahn, Y. M. Kim, S. J. Kwon, S. Y. Yoon, H. J. Kang and S. J. Chung, Metal-induced redshift of optical spectra of gold nanoparticles: An instant, sensitive, and selective visual detection of lead ions, *Int. Biodeterior. Biodegrad.*, 2019, **144**, 104740, DOI: 10.1016/j.ibiod.2019.104740.

19 Z. Chen, Z. Zhang, J. Qi, J. You, J. Ma and L. Chen, Colorimetric detection of heavy metal ions with various chromogenic materials: Strategies and applications, *J. Hazard Mater.*, 2023, **441**, 129889, DOI: 10.1016/j.jhazmat.2022.129889.

20 R. M. Tripathi and S. J. Chung, Phytosynthesis of palladium nanoclusters: an efficient nanozyme for ultrasensitive and selective detection of reactive oxygen species, *Molecules*, 2020, **25**(15), 3349, DOI: 10.3390/molecules25153349.

21 S. Bansal, A. Deshwal, P. Sharma, R. N. Pudake, F. A. Sheikh and R. M. Tripathi, Opportunities and trends in therapeutics application of nanozymes, *Nanozymes*, 2024, **1**, 139–156, DOI: 10.1016/B978-0-443-13788-4.00005-4.

22 R. M. Tripathi and S. J. Chung, Ultrasensitive and selective colorimetric detection of uric acid using peroxidase mimetic activity of biogenic palladium nanoparticles, *Luminescence*, 2023, **38**(7), 1330–1338, DOI: 10.1002/bio.4425.

23 D. Luo, X. Huang, B. Liu, W. Zou and Y. Wu, Facile colorimetric nanozyme sheet for the rapid detection of glyphosate in agricultural products based on inhibiting peroxidase-like catalytic activity of porous Co3O4 nanoplates, *J. Agric. Food Chem.*, 2021, **69**(11), 3537–3547, DOI: 10.1021/acs.jafc.0c08208.

24 S. Ghayyem, A. Swaidan, A. Barras, M. Dolci, F. Faridbod, S. Szunerits and R. Boukherroub, Colorimetric detection of chromium (VI) ion using poly (N-phenylglycine) nanoparticles acting as a peroxidase mimetic catalyst, *Talanta*, 2021, **226**, 122082, DOI: 10.1016/j.talanta.2021.122082.

25 R. D. Isho, N. M. Mohammad and K. M. Omer, Enhancing enzymatic activity of Mn@ Co3O4 nanosheets as mimetic nanozyme for colorimetric assay of ascorbic acid, *Anal. Biochem.*, 2022, **654**, 114818, DOI: 10.1016/j.ab.2022.114818.

26 M. Bilal, N. Khaliq, M. Ashraf, N. Hussain, Z. Baqar, J. Zdarta, T. Jesionowski and H. M. Iqbal, Enzyme mimic nanomaterials as nanozymes with catalytic attributes, *Colloids Surf., B*, 2023, **221**, 112950, DOI: 10.1016/j.colsurfb.2022.112950.

27 E. Sánchez-Tirado, P. Yáñez-Sedeño and J. M. Pingarrón, Carbon-based enzyme mimetics for electrochemical biosensing, *Micromachines*, 2023, **14**(9), 1746, DOI: 10.3390/mi14091746.

28 G. L. Wang, X. F. Xu, L. H. Cao, C. H. He, Z. J. Li and C. Zhang, Mercury (ii)-stimulated oxidase mimetic activity of silver nanoparticles as a sensitive and selective mercury (ii) sensor, *RSC Adv.*, 2014, **4**(12), 5867–5872, DOI: 10.1039/c3ra45226c.

29 R. M. Tripathi and S. J. Chung, Eco-friendly synthesis of SnO2-Cu nanocomposites and evaluation of their peroxidase mimetic activity, *Nanomaterials*, 2021, **11**(7), 1798, DOI: 10.3390/nano11071798.

30 J. Mu, Y. Wang, M. Zhao and L. Zhang, Intrinsic peroxidase-like activity and catalase-like activity of Co 3 O 4 nanoparticles, *Chem. Commun.*, 2012, **48**(19), 2540–2542, DOI: 10.1039/c2cc17013b.

31 Y. Sun, L. Chen, Y. Bao, Y. Zhang, J. Wang, M. Fu, J. Wu and D. Ye, The applications of morphology controlled ZnO in catalysis, *Catalysts*, 2016, **6**(12), 188, DOI: 10.3390/catal6120188.

32 A. Wang, W. Quan, H. Zhang, H. Li and S. Yang, Heterogeneous ZnO-containing catalysts for efficient biodiesel production, *RSC Adv.*, 2021, **11**(33), 20465–20478, DOI: 10.1039/d1ra03158a.

33 A. Deshwal and R. M. Tripathi, Palladium-powered nanozymes: A paradigm shift in precision medicine, *Chem. Eng. J.*, 2025, **6**, 168043, DOI: 10.1016/j.cej.2025.168043.

34 R. M. Tripathi and S. J. Chung, Reclamation of hexavalent chromium using catalytic activity of highly recyclable biogenic Pd (0) nanoparticles, *Sci. Rep.*, 2020, **10**(1), 640, DOI: 10.1038/s41598-020-57548-z.

35 R. M. Tripathi and S. J. Chung, Prodigious catalytic activity towards reduction of 4-hydroxynitrobenzene sodium salt using one-pot synthesized ZnO-Pd nanobolts, *Surf. Interfaces*, 2024, **44**, 103580, DOI: 10.1016/j.surfin.2023.103580.

36 E. A. Kukreja, R. M. Tripathi and S. J. Chung, Colorimetric and smartphone-based dual modality sensing platform for detection of ascorbic acid, *Sens. Actuators, A*, 2025, **389**, 116573, DOI: 10.1016/j.sna.2025.116573.

37 R. M. Tripathi, D. Ahn, Y. M. Kim and S. J. Chung, Enzyme mimetic activity of ZnO-Pd nanosheets synthesized *via* a green route, *Molecules*, 2020, **25**(11), 2585, DOI: 10.3390/molecules25112585.

38 L. Ren, W. Zhou, B. Sun, H. Li, P. Qiao, Y. Xu, J. Wu, K. Lin and H. Fu, Defects-engineering of magnetic γ-Fe2O3 ultrathin nanosheets/mesoporous black TiO2 hollow sphere heterojunctions for efficient charge separation and the solar-driven photocatalytic mechanism of tetracycline degradation, *Appl. Catal., B*, 2019, **240**, 319–328, DOI: 10.1016/j.apcatb.2018.08.033.

39 J. Qi, Y. Wan, J. Li, G. Jiang, J. Wang, Y. Ozaki and F. Pi, A competitive dual-mode for tetracycline antibiotics sensing based on colorimetry and surface-enhanced Raman scattering, *Biosens. Bioelectron.*, 2025, **272**, 117114, DOI: 10.1016/j.bios.2024.117114.

40 Y. Wang, Y. Sun, H. Dai, P. Ni, S. Jiang, W. Lu, Z. Li and Z. Li, A colorimetric biosensor using Fe3O4 nanoparticles for highly sensitive and selective detection of tetracyclines, *Sens. Actuators, B*, 2016, **236**, 621–626, DOI: 10.1016/j.snb.2016.06.029.

41 B. Liu, H. Zhu, R. Feng, M. Wang, P. Hu, J. Pan and X. Niu, Facile molecular imprinting on magnetic nanozyme surface for highly selective colorimetric detection of tetracycline, *Sens. Actuators, B*, 2022, **370**, 132451, DOI: 10.1016/j.snb.2022.132451.

42 H. Chen, Z. Wang, Q. Shi, W. Shi, Y. Lv and S. Liu, A Colorimetric and Fluorescent Dual-Mode Sensor Based on a Smartphone-Assisted Laccase-like Nanoenzyme for the Detection of Tetracycline Antibiotics, *Nanomaterials*, 2025, **15**(3), 162, DOI: 10.3390/nano15030162.

43 Z. Zhang, Y. Tian, P. Huang and F. Y. Wu, Using target-specific aptamers to enhance the peroxidase-like activity of gold nanoclusters for colorimetric detection of tetracycline antibiotics, *Talanta*, 2020, **208**, 120342, DOI: 10.1016/j.talanta.2019.120342.

44 X. Guo, H. Sun, Y. Yang, W. Zhong, M. Wang, G. Wang and Y. Zhang, Nanozyme-based colorimetric and smartphone imaging advanced sensing platforms for tetracycline detection and removal in food, *Talanta*, 2025, **283**, 127028, DOI: 10.1016/j.talanta.2024.127028.

45 H. Shang, X. Zhang, M. Ding, A. Zhang and C. Wang, A smartphone-assisted colorimetric and photothermal probe for glutathione detection based on enhanced oxidase-mimic CoFeCe three-atom nanozyme in food, *Food Chem.*, 2023, **423**, 136296, DOI: 10.1016/j.foodchem.2023.136296.

